Chapter 7

Effect of Unsteady-State Heat Flow Regime Solidification on the Mechanical Properties of Al-5Cu-5Si-5Mg-5Zn-1Zr Alloy

Emin Çadırlı[1]

Uğur Büyük[2]

Hasan Kaya[3]

Erkan Üstün[4]

Abstract

This study comprehensively investigates the impact of unsteady-state heat flow regime solidification on the thermal behavior and mechanical properties of the multicomponent Al-5Cu-5Si-5Mg-5Zn-1Zr (wt.%) alloy. The alloy was solidified in the unsteady-state heat flow regime at a cooling rate range of approximately (0.88–2.77 °C/s) using a custom-built solidification furnace equipped with eight thermocouples. Eutectic spacing (λ) decreased from 20 μm to 6 μm with increasing cooling rates, directly correlating with enhanced mechanical properties. The highest microhardness (HV=177.5 kg/mm^2), compressive strength (σc=556.9 MPa), and compressive yield strength (σy=385.5 MPa) were achieved at the fastest cooling rate (2.77°C/s). These findings underscore the critical role of cooling rate optimization in achieving superior mechanical performance for aerospace and automotive applications.

1 Prof. Dr., Niğde Ömer Halisdemir University, Faculty of Science, Department of Physics, Niğde, Turkey, ecadirli@gmail.com, ORCID: 0000-0002-8085-9733

2 Prof. Dr., Erciyes University, Faculty of Education, Department of Mathematics and Science Education, Kayseri, Turkey, buyuk@erciyes.edu.tr, ORCID: 0000-0002-6830-8349

3 Prof. Dr., Erciyes University, Faculty of Education, Department of Mathematics and Science Education, Kayseri, Turkey, hasankaya@erciyes.edu.tr, ORCID: 0000-0003-3529-9762

4 Dr., Niğde Ömer Halisdemir University, Institute of Science, Department of Physics, Niğde, Turkey, erkanustun_07@hotmail.com, ORCID: 0000-0002-7745-396X

https://doi.org/10.58830/ozgur.pub770.c3185

1. Introduction

Aluminum alloys have revolutionized modern engineering by offering an unparalleled combination of lightweight properties, corrosion resistance, and recyclability. Their dominance in industries such as aerospace, automotive, and construction stems from their ability to meet stringent performance demands while reducing energy consumption and carbon footprints. For instance, replacing traditional steel components with aluminum alloys in automotive structures can reduce vehicle weight by 40–50%, leading to a 6–8% improvement in fuel efficiency and a proportional reduction in greenhouse gas emissions. However, as industries push toward higher efficiency and sustainability, the demand for advanced aluminum alloys with superior mechanical and thermal properties has intensified.

Multicomponent aluminum alloys, particularly those in the Al-Cu-Si-Mg system, have emerged as frontrunners due to their capacity to integrate multiple strengthening mechanisms. Copper enhances strength through precipitation hardening, silicon improves castability and wear resistance, magnesium contributes to solid solution strengthening, and zinc refines grain boundaries. Despite these advantages, the performance of such alloys is highly sensitive to solidification conditions. Conventional casting methods often result in microstructural heterogeneity, including coarse dendritic structures, segregated intermetallic phases, and porosity, which compromise mechanical integrity. For example, uneven cooling rates can lead to localized stress concentrations, reducing fatigue life by up to 30% in critical components like engine blocks or aircraft fuselage frames.

A critical challenge in multicomponent alloy design lies in balancing compositional complexity with microstructural control. The addition of transition elements like zirconium (Zr) has shown promise in addressing this issue. Zirconium, even in trace amounts (0.1–1 wt.%), forms thermally stable Al_3Zr precipitates that inhibit grain boundary migration and recrystallization, thereby enhancing high-temperature stability. Recent studies by Shaha et al. (2014) demonstrated that Zr additions in Al-Si-Cu-Mg alloys improved tensile strength by 18% and creep resistance by 25% at 200°C. Similarly, Sandoval et al. (2014) reported that Zr-modified Al-Si-Cu-Mg alloys exhibited a 40% reduction in dendritic arm spacing under rapid cooling conditions, directly correlating with a 15% increase in hardness. These findings underscore Zr's dual role as a grain refiner and precipitation strengthener, making it a strategic addition for advanced alloy systems. The solidification process itself is a pivotal factor in determining microstructure and properties. Traditional steady-state cooling methods

often fail to replicate the dynamic thermal gradients encountered in industrial casting, leading to discrepancies between laboratory-scale and real-world performance. Unsteady-state heat flow regimes, characterized by spatially and temporally varying cooling rates, offer a more realistic framework for studying solidification behavior. For instance, Rosso et al. (2022) observed that non-uniform cooling in Al-Si alloys promoted finer eutectic structures and reduced porosity by 22% compared to uniform cooling. However, systematic studies on multicomponent Al alloys under such conditions remain scarce, particularly for systems incorporating Zn and Zr.

This study addresses these gaps by investigating the Al-5Cu-5Si-5Mg-5Zn-1Zr alloy, a novel composition designed for high-stress applications in aerospace and automotive sectors. The inclusion of 5 wt.% Zn aims to enhance fluidity and corrosion resistance, while 1 wt.% Zr targets microstructural stabilization through Al_3Zr precipitation. The primary objectives are:

i. To characterize the microstructure and thermal properties of the alloy under unsteady-state heat flow conditions.

ii. To quantify the relationship between cooling rate and mechanical performance.

iii. To establish a predictive model for optimizing industrial solidification processes.

In the previous study, the effect of steady-state heat flow regime solidification on the microstructural and phase properties of multicomponent Al-5Cu-5Si-5Mg-5Zn-1Zr (wt.%) alloy was investigated (Kaya et al. (2024)). The novelty of this work lies in its holistic approach to linking non-uniform cooling dynamics with mechanical behavior in a Zr-modified multicomponent system. By employing a custom-built solidification furnace with eight thermocouples, this study captures real-time thermal gradients rarely replicated in prior research. Furthermore, the integration of Zn and Zr addresses a critical industry need for alloys that combine high strength with manufacturability, particularly in complex die-cast components.

2. Materials and Methods

2.1. Alloy Design and Preparation

The Al-5Cu-5Si-5Mg-5Zn-1Zr (wt.%) alloy was formulated using high-purity raw materials: aluminum (99.99%), copper (99.95%), silicon (99.9%), magnesium (99.8%), zinc (99.9%), and zirconium (99.5%). The

nominal composition was verified via inductively coupled plasma optical emission spectroscopy (ICP-OES) (Table 1), with deviations limited to $< \pm 0.3$ wt.% for all elements.

Table 1. Nominal and measured composition of the alloy (wt.%).

Element	Nominal	Measured
Al	79.0	79.2 ± 0.2
Cu	5.0	4.9 ± 0.1
Si	5.0	5.1 ± 0.2
Mg	5.0	4.8 ± 0.1
Zn	5.0	4.7 ± 0.3
Zr	1.0	1.1 ± 0.05

2.2. Melting and Casting

Melting was conducted in a vacuum melting furnace under an argon atmosphere (99.999% purity) to minimize oxidation. The process involved:

i. **Charging:** Aluminum ingots were loaded into a graphite crucible and heated to 750°C

ii. **Alloying:** Cu, Si, Mg, Zn, and Zr were added sequentially for 15 minutes after each addition.

iii. **Degassing:** High-purity argon was bubbled through the melt for 10 minutes to remove dissolved hydrogen.

iv. **Casting:** The molten alloy was poured into preheated (300°C) graphite molds with dimensions of Ø30 mm×150 mm (Fig. 1a).

The graphite crucible, funnel and vacuum melting furnace used in master alloy preparation are given in Fig.1.

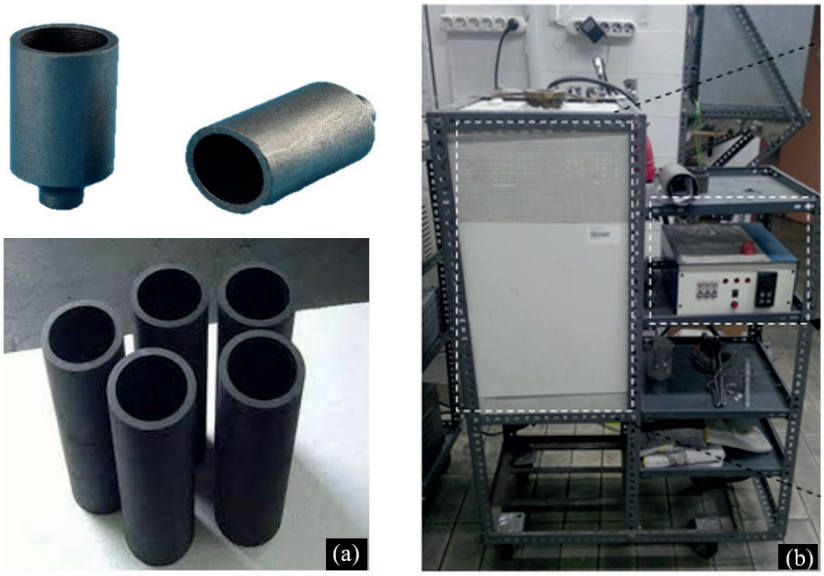

Fig. 1. (a) Graphite molds and funnels, (b) Vacuum melting furnace schematic

2.3. Unsteady-State Solidification Setup

A vertical solidification furnace was designed to impose controlled thermal gradients (Fig. 2). Key components included:

- **Cooling System:** A water-cooled tank (Ø50 mm×20 mm) at the mold base, maintained at 10°C via a recirculating chiller.
- **Thermal Monitoring:** Eight K-type thermocouples (T1–T8, ±0.5°C accuracy) embedded at 1 cm intervals along the mold height
- **Data Acquisition:** A National Instruments TC-08 data logger recorded temperature at 10 Hz, synchronized with LabVIEW software.

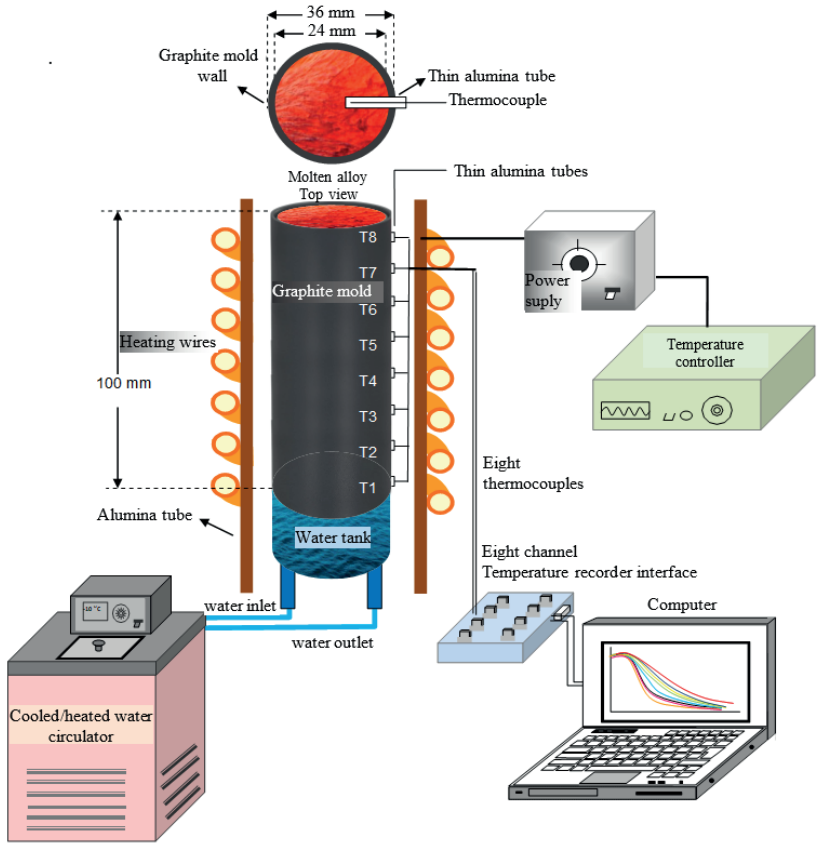

Fig. 2. Unsteady-state heat flow experimental setup

2.4. Microstructural Characterization

Samples were sectioned longitudinally and transversely using a water-cooled abrasive cutter (Struers Secotom-15). Polishing was performed on a Struers LaboPol-5 system with diamond suspensions (9 μm to 0.25 μm). Etching used Keller's reagent (2% HF, 3% HCl, 5% HNO_3, 90% H_2O) for 10–15 seconds. Microstructure and phase analyses are given in detail in the authors' previous studies (Kaya et al. (2024)).

2.5. Thermal Anaysis and Mechanical Testing

Differential scanning calorimetry (DSC) was performed on a Perkin Elmer Pyris Diamond system. Samples (30 ± 0.5 mg) were heated from 25°C to 800 °C at 20°C/min under nitrogen flow (50 mL/min). Melting

onset (T_m), peak temperature, enthalpy (ΔH), and specific heat (C_p) were derived from heat flow curves.

Vickers microhardness (HV) was measured using a Future Tech FM-700 tester with a 500 gf load and 15 s dwell time. Samples solidified at different cooling rates were connected to the testing device in order and many measurements were made from different areas. Cylindrical specimens (Ø5 mm × 7 mm) were machined parallel to the solidification direction. A Shimadzu AG-IS universal tester applied uniaxial compression at 1 mm/min strain rate until 30% deformation. Stress-strain curves determined compressive strength (σ_c) and yield strength (σ_y) at 0.2% offset.

3. Results and Discussions

The experimental investigation of the Al-5Cu-5Si-5Mg-5Zn-1Zr alloy solidified under unsteady-state heat flow conditions revealed significant variations in microstructure, thermal behavior, and mechanical properties as a function of cooling rate and position. The results are presented in detail below, integrating quantitative data, visual observations, and comparative analyses.

3.1. Cooling Rate Distributions

The unsteady-state solidification process generated significant spatial variations in cooling rates along the ingot height. As shown in Fig. 3 and Table 2, cooling rates decreased exponentially from the mold base (T1: 2.77 ± 0.12°C/s) to the top (T8: 0.88 ± 0.05°C/s).

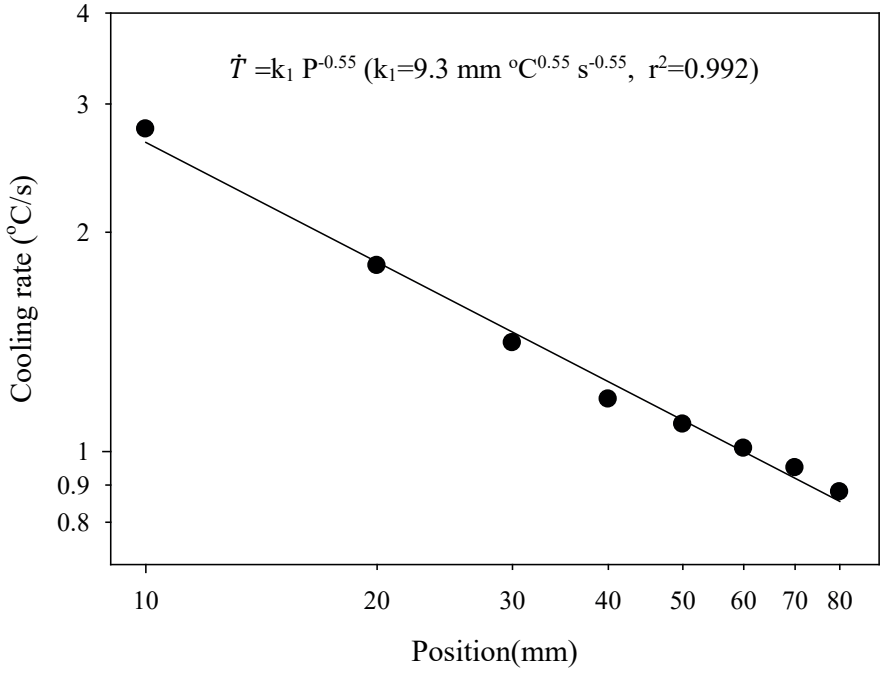

Fig. 3. Change of cooling rates according to the position from the sample base

Table 2. Cooling rates at different positions (heights from the sample base).

Distance from base (cm)	Cooling rate (°C/s)	Standard deviation
1 (T1-Region 1)	2.77	±0.12
2 (T2)	1.80	±0.09
3 (T3)	1.41	±0.07
4 (T4)	1.18	±0.08
5 (T5)	1.09	±0.06
6 (T6)	1.01	±0.05
7 (T7)	0.95	±0.04
8 (T8-Region 8)	0.88	±0.05

As seen in Fig. 3, the cooling rate decreased to approximately one third of the value as we went upwards from the sample base. From the relation between Ṫ and P, it is seen that Ṫ varies inversely proportional to the exponential value of P of 0.55. This value is in good agreement with the value of 0.56 obtained by Rosso et al. (2022) for the multi-Al alloy.

3.2. Thermal Properties

Fig. 4 shows the DSC curve of the alloy sample studied. Since the alloy studied is a multi-alloy system, it contains intermetallic phases such as Al_2Cu and Mg_2Si as mentioned in the previous study (Kaya et al. (2024)). In this graph, the red arrow indicates the onset temperature. The first peak at 503.8°C corresponds to the melting of the Al_2Cu eutectic phase, the second peak at 546.6°C corresponds to the melting of the Mg_2Si intermetallic phase, and finally, the third peak at 588.1°C indicates the complete melting of the α-Al primary phase. The findings of Sandoval et al. (2014) support our obtained data. These researchers determined that Al_2Cu melts at 500°C, Mg_2Si at 540°C, and α-Al at 597°C, in the same order. Using the data obtained from this curve, the initial melting onset temperature (T_{onset}), enthalpy (ΔH), and specific heat capacity (Cp) were calculated as 491.3°C, 301 J/g, and 0.658 J/g°C, respectively. Kageyama and Morita (2023) found an enthalpy value of 321 J/g for the Al-Cu-Si-Mg-Zn alloy.

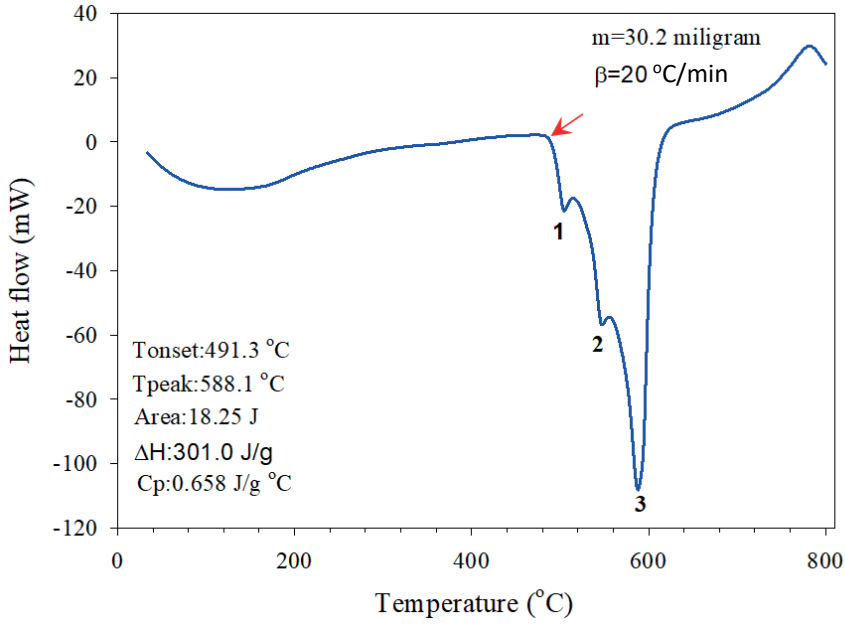

Fig. 4. DSC curve of the studied sample and the obtained thermal parameters.

3.3. Mechanical Properties

3.3.1. Microhardness

The variations in microhardness values with respect to the distance from the base, cooling rate, and eutectic spacing are presented in Fig. 5. As seen in Fig. 5(a), HV exhibited an inverse proportional change with the distance from the base (P) following an exponent of 0.28.

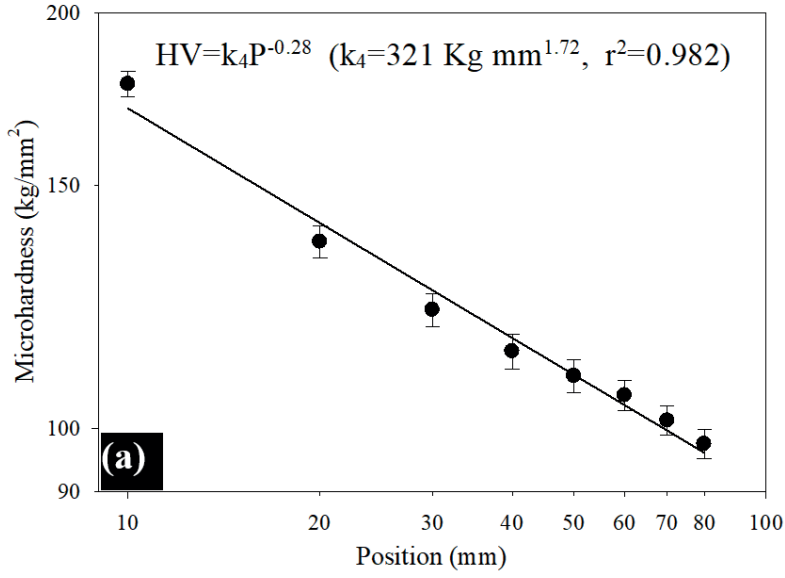

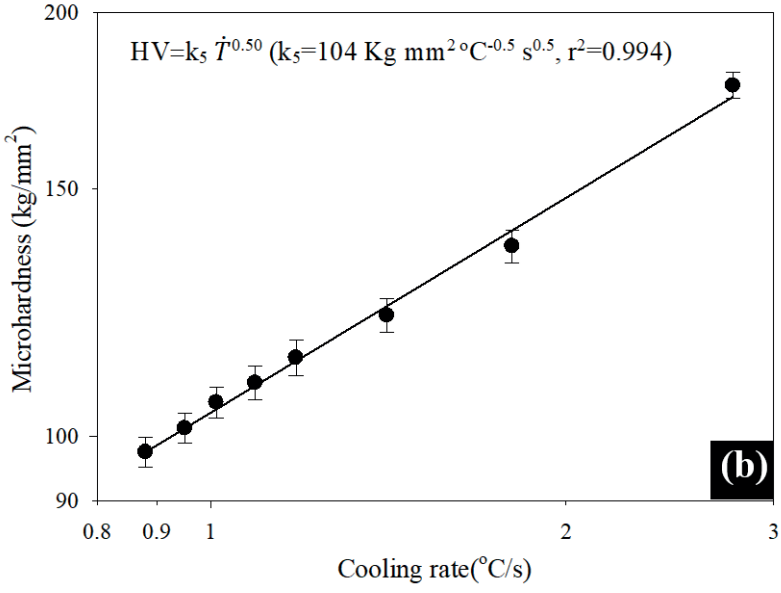

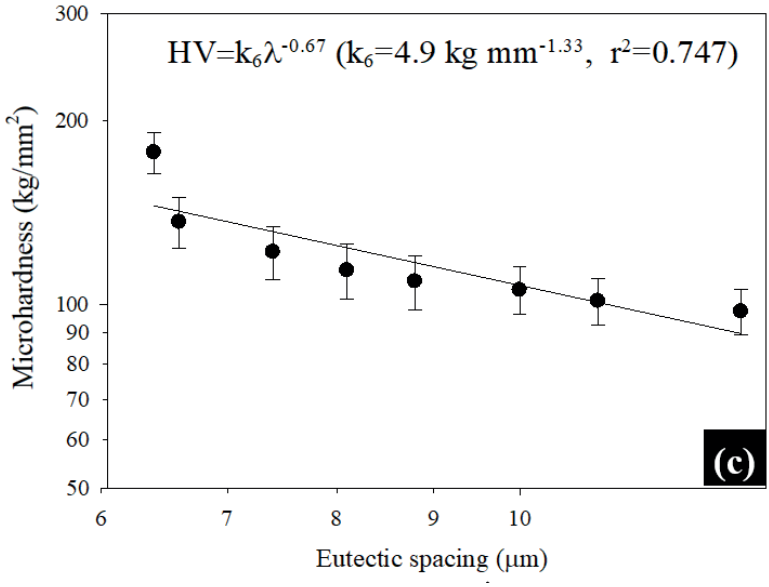

Fig. 5. (a) HV-P change, (b) HV-Ṫ change, (c) HV-λ change

As seen in Fig. 5(b), as the cooling rate increases from 0.88 °C/s to 2.77 °C/s, the HV value increases from 97 kg/mm² to 177 kg/mm². The experimental correlation obtained from the graph indicates that HV is directly proportional to Ṫ with an exponent of 0.5. In Fig. 5(c), it is observed that as the eutectic spacing increases, the HV value decreases. The experimental correlation provided in the graph shows that HV is inversely proportional to λ with an exponent of 0.67. Araujo et al. (2016) reported that HV in Al-Cu-Si alloys exhibits an inverse proportionality to λ with an exponent of 0.55. Baek et al. (2017) subjected an Al-10Mg-10Si-5Cu-5Zn multi-alloy system to a heat treatment at 440 °C for 10 hours and obtained an approximate microhardness value of 140 kg/mm². Chaskis et al. (2022) conducted a heat treatment at 200 °C for 24 hours on an Al-13.3Mg-23.8Zn-9.6Cu-6Si multi-component Al alloy, achieving a microhardness value of approximately 171 kg/mm². Sanchez et al. (2021) reported a microhardness value of 159 kg/mm² for the as-cast state of the Al-5Mg-5Sn-5Zn-5Ti alloy at room temperature.

3.3.2. Compressive Strength

Fig. 6 shows the compression stress-strain curves of samples solidified at different cooling rates at room temperature. As observed from these curves, both the compressive strength and compressive yield strength increase as the

cooling rate increases. The lowest compression, approximately 17%, was observed in the sample solidified at a cooling rate of 0.95 °C/s (Region 7), while the highest compression, approximately 26%, was observed in the sample solidified at a cooling rate of 1.80 °C/s (Region 2). Fig. 7 presents the variations in compressive strength values concerning the distance from the sample base (P), cooling rate ($\dot{T}$), and eutectic spacing (λ).

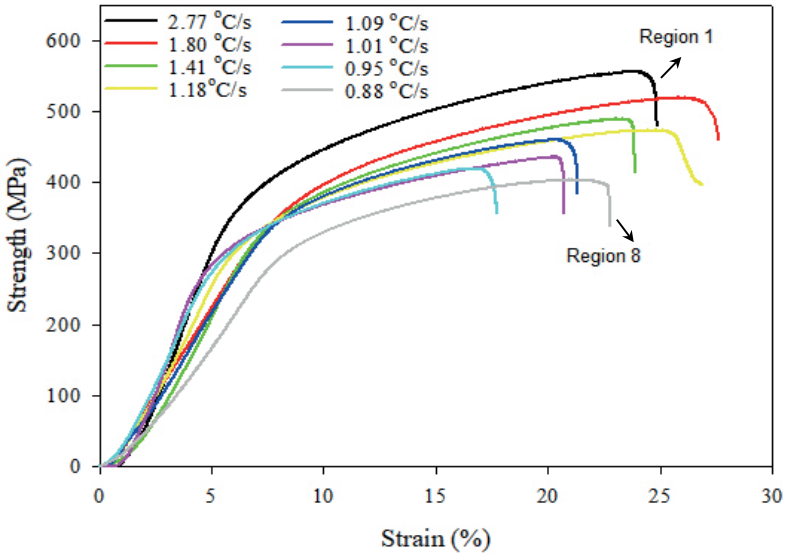

Fig. 6. Compressive stress-strain curves

As observed from the experimental correlations obtained in Fig. 7(a), the compressive strength (σ_c) and compressive yield strength (σ_y) exhibit an inverse relationship with P, following exponent values of 0.16 and 0.18, respectively.

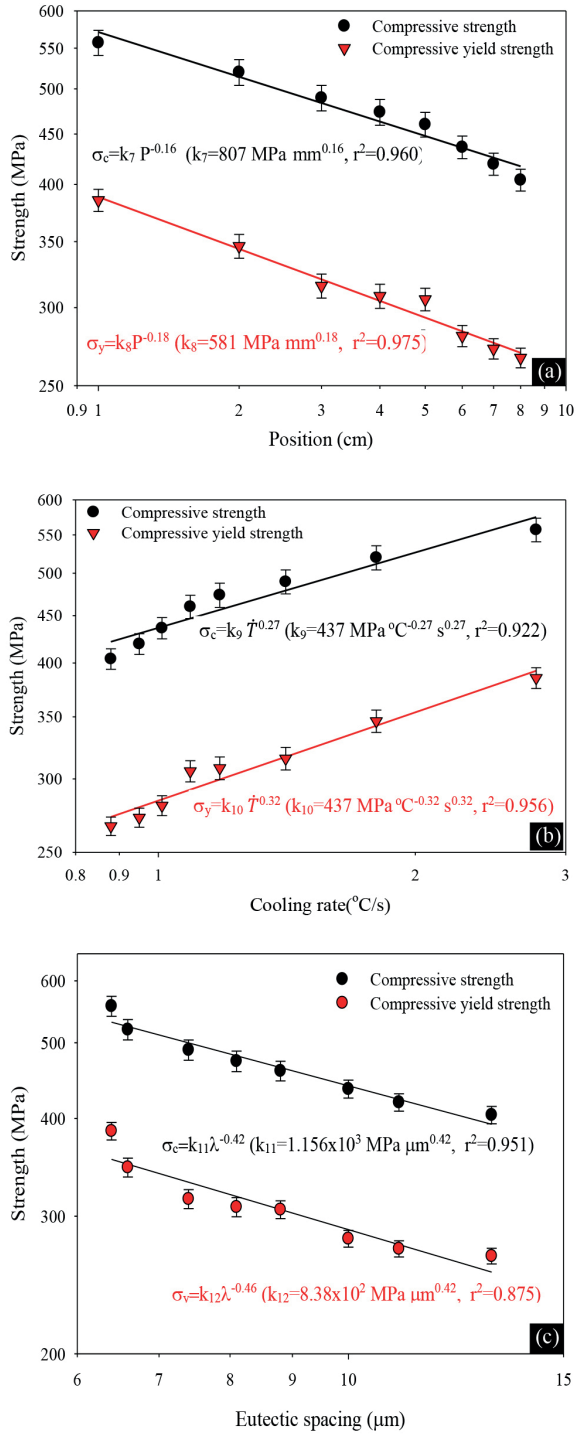

Fig. 7. (a) (σc, σy)-P change, (b) (σc, σy)-Ṫ change, (c) (σc, σy)-λ change

Fig. 7(b) illustrates the correlation between cooling rate and compressive properties, specifically compressive strength (σ_c) and compressive yield strength (σ_y). As the cooling rate ($\dot{T}$) increased from 0.88 °C/s to 2.77 °C/s, both compressive strength and compressive yield strength exhibited a corresponding increase, rising from 404 MPa and 266 MPa to 556 MPa and 385 MPa, respectively. The relationships between cooling rate and these mechanical properties were found to be directly proportional, with σ_c and σ_y scaling with cooling rate to the power of 0.27 and 0.32, respectively. Conversely, Fig. 7(c) demonstrates the inverse relationship between eutectic spacing and compressive properties. An increase in eutectic spacing resulted in a decrease in both compressive strength and compressive yield strength. Experimentally derived correlations indicated an inverse proportionality between σ_c and σ_y with eutectic spacing (λ), characterized by exponents of 0.42 and 0.46, respectively.

To contextualize these findings, the compressive strength and compressive yield strength values obtained in this study are compared with literature data for similar multicomponent aluminum alloys. Baek et al. (2017) reported compressive strength and compressive yield strength values of 414 MPa and 369 MPa, respectively, for a cast Al-10Mg-10Si-5Cu-5Zn alloy. Chaskis et al. (2022) measured a compressive strength of 588 MPa for a cast Al-13.3Mg-23.8Zn-9.6Cu-6Si multicomponent aluminum alloy. Sanchez et al. (2021) determined the compressive strength, compressive yield strength, and compressive strain (%) of a cast medium-entropy Al-5Mg-5Sn-5Zn-5Ti alloy at room temperature to be 563 MPa, 420 MPa, and 12%, respectively. In another study, Sanchez et al. (2019) investigated a medium-entropy Al-5Cu-5Mg-10Si-5Zn-5Zr alloy produced via induction furnace, reporting cast-state compressive strength, compressive yield strength, and compressive strain values of 633 MPa, 565 MPa, and 4%, respectively. Shao et al. (2018) synthesized a medium-entropy Al-14Mg-2.7Zn-2.7Cu-0.6Si alloy using an induction furnace under a high-purity argon atmosphere and reported compressive strength, compressive yield strength, and compressive strain of 498 MPa, 203 MPa, and 13.8%, respectively, for the cast alloy.

4. Conclusion

This study systematically investigated the effects of unsteady-state heat flow regime solidification on the microstructure, thermal properties, and mechanical performance of the multicomponent Al-5Cu-5Si-5Mg-5Zn-1Zr alloy. The key findings are summarized as follows:

1. During free solidification under an unstable heat flow regime, the bottom part of the sample solidified at a cooling rate of 2.77 °C/s, while the top part solidified at a cooling rate of 0.88 °C/s. There is approximately a threefold difference in cooling rates between the top region (Region 8) and the bottom region (Region 1)
2. For the studied alloy, the initial melting temperature was determined as 491.3 °C, the final melting temperature as 588.1 °C, the enthalpy as 301 J/g, and the specific heat capacity as 0.658 J/g °C.
3. Due to the higher cooling rate at the bottom part of the sample, the highest mechanical properties were obtained as HV=177.5 kg/mm^2, σ_c=556.9 MPa, and σ_y=385.5 MPa. In contrast, at the top part of the sample, where the cooling rate was relatively lower, the values were HV=97.4 kg/mm^2, σ_c=404.1 MPa, and σ_y=266.7 MPa. Additionally, the minimum compression strain (~17%) was observed in Region 7, while the maximum compression strain (~26%) was found in Region 2. The final physical properties of the material are influenced by several factors, including the microstructure (size, shape, and composition of different phase components), the presence of precipitate phases (composition, distribution, and grain size), and the interactions between these phases. Silicon alone contributes minimally to the strength of aluminum casting alloys. However, in this study, its combination with Mg and Cu facilitated the formation of precipitate phases such as Al_2Cu and Mg_2Si during solidification, significantly enhancing both hardness and compressive properties. Moreover, the presence of a small amount of Zr in the alloy inhibited dislocation movement by forming coherent grains, preventing recrystallization.

Acknowledgements

This work was financially supported by **Erciyes University Scientific Research Projects Coordination Unit** under grant number **FBA-2023-12765**. The authors extend their gratitude to the *Erciyes Universty Technology Research And Application Center* for providing access to SEM and XRD facilities.

References

Araujo, R. L. M., Kikuchi, R. H. L., Barros, A. S., Gomes, L. G., Moutinho, D. J. C., Gonçalves, F. A., Moreira, A. L. S., & Rocha, O. F. L. (2016). Influence of upward and horizontal growth direction on microstructure and microhardness of an unsteady-state directionally solidified Al-Cu-Si alloy. *Revista Matéria, 21*(1), 261–269.

https://doi.org/10.1590/S1517-707620160001.0024

Baek, E. J., Ahn, T. Y., Jung, J. G., Lee, J. M., Cho, Y. R., & Euh, K. (2017). Effects of ultrasonic melt treatment and solution treatment on the microstructure and mechanical properties of low-density multicomponent Al70Mg10Si10Cu5Zn5 alloy. *Journal of Alloys and Compounds, 696*, 450–459.

https://doi.org/10.1016/j.jallcom.2016.11.305

Chaskis, S., Stachouli, E., Gavalas, E., Bouzouni, M., & Papaefthymiou, S. (2022). Microstructure, phase formation and heat-treating of novel cast Al-Mg-Zn-Cu-Si lightweight complex concentrated aluminum based alloy. *Materials, 15*(9), 3169.

https://doi.org/10.3390/ma15093169

Kaya, H., Çadırlı, E., Büyük, U., & Üstün, E. (2024). Microstructural evolution and phase formation of Al-5Cu-5Si-5Mg-5Zn-1Zr alloy freely solidified in the unsteady state heat flow regime. In M. M. Türkoğlu (Ed.), *Interdisciplinary studies on contemporary research practices in engineering- VII* (pp. 45–60). Özgür Publications.

https://doi.org/10.58830/ozgur.pub575.c2359

Kageyama, Y., & Morita, K. (2023). Compositional and thermophysical study of Al–Si- and Zn–Al–Mg-based eutectic alloys for latent heat storage. *High Temperature Materials and Processes, 42*(1), 20220269.

https://doi.org/10.1515/htmp-2022-0269

Rosso, E., Santos, C. A., & Garcia, A. (2022). Microstructure, Hardness, Tensile Strength, and Sliding Wear of Hypoeutectic Al–Si Cast Alloys with Small Cr Additions and Fe-Impurity Content. *Advanced Engineering Materials, 24*(8), 2001552.

https://doi.org/10.1002/adem.202001552

Sanchez, J. M., Pascual, A., Vicario, I., Albizuri, J., Guraya, T., & Galarraga, H. (2021). Microstructure and phase formation of novel Al80Mg5Sn-5Zn5X5 light-weight complex concentrated aluminum alloys. Metals, 11(12), 1944.

https://doi.org/10.3390/met11121944

Sanchez, J. M., Vicario, I., Albizuri, J., Guraya, T., & Acuña, E. M. (2019). Design, microstructure and mechanical properties of cast medium entropy aluminium alloys. *Scientific reports, 9*(1), 6792.

https://doi.org/10.1038/s41598-019-43329-w

Hernandez-Sandoval, J., Samuel, A. M., Valtierra, S., & Samuel, F. H. (2014). Ni-And Zr-Based Intermetallics in Al–Si–Cu–Mg Cast Alloys. *Metallography, Microstructure, and Analysis, 3,* 408-420.

https://doi.org/10.1007/s13632-014-0164-2

Shaha, S. K., Czerwinski, F., Kasprzak, W., & Chen, D. L. (2014). Tensile and compressive deformation behavior of the Al-Si-Cu-Mg cast alloy with additions of Zr, V and Ti. *Materials & Design, 59*, 352–358.

https://doi.org/10.1016/j.matdes.2014.02.060

Shao, L., Zhang, T., Li, L., Zhao, Y., Huang, J., Liaw, P. K., & Zhang, Y. (2018). A low-cost lightweight entropic alloy with high strength. *Journal of Materials Engineering and Performance, 27*(12), 6648–6656.

https://doi.org/10.1007/s11665-018-3720-0